Stacking−Unstacking Dynamics of Oligodeoxynucleotide Trimers†

John M. Jean* and Kathleen B. Hall*

Department of Biochemistry and Molecular Biophysics, Washington University School of Medicine, St. Louis, Missouri 63110

Received February 10, 2004; Revised Manuscript Received May 7, 2004

ABSTRACT: The structure and dynamics of DNA trimers are experimentally assessed using the fluorescent purine analogue 2-aminopurine (2AP), incorporating 2AP between purine and pyrimidine bases to form $^{5'}$dXp2APpY$^{3'}$ molecules. Circular dichroism and fluorescence quenching of the 2AP show that the bases are stacked; at the same time, fluorescence decay lifetimes are heterogeneous, indicative of conformational sampling. 2AP does not exhibit the long fluorescence decay time characteristic of the free nucleoside, suggesting that its motions in the trimers bring it into proximity of the neighboring bases, resulting in efficient charge transfer and average fluorescence lifetimes on the order of 1−2 ns.

The structure and dynamics of single-stranded nucleic acids will determine their ease of access by proteins and other nucleic acids. While single-stranded DNA sequences seldom appear in most biological systems, RNA molecules typically contain single-stranded regions. The termini of RNA molecules are often sites of interactions with proteins [e.g., the poly(A) tail and the 5′ UTR of metazoan mRNAs and the CCA 3′ tail of tRNAs] or with RNAs (e.g., the 5′ conserved sequence of U1 snRNA, the 3′ end of 16S rRNA with its Shine−Delgarno sequence, and the termini of group I introns). These termini will have unique physical properties, including more conformational flexibility with more rapid dynamic motions, than those of internal single-stranded sequences, for the latter will be constrained to some extent by their boundaries and flanking structures.

To study the solution properties of nucleic acid termini, DNA trimers were synthesized that contained an internal 2-aminopurine (2AP) fluorescent nucleotide. These short oligodeoxynucleotides are predicted to represent the physical properties of both DNA and RNA, since their length will preclude extensive and stable stacking into the canonical A- or B-form structures. Single-stranded nucleic acids are not random coil polymers, however; circular dichroism spectra show signals indicative of helical base stacking, and thermal melting profiles show a gradual increase in absorbance with increasing temperature, consistent with the hypochromicity associated with stacked nucleobases but without the cooperativity of a duplex. The DNA trimers used for our experiments will also mimic the termini of RNA molecules and so provide a description of how these ends might appear in solution.

The fluorescent nucleotide 2-aminopurine (2AP)[1] has been widely used as a probe of local structure of nucleic acids due to its ability to pair with thymine/uracil and the sensitivity of its fluorescence properties to stacking interactions with neighboring bases. Free 2AP in solution has a fluorescence quantum yield of 0.68 at pH 7 in 100 mM NaCl at 25 °C (*1*), but in the context of a strand (single strand or duplex) its fluorescence is quenched. It is now well accepted that the quenching of 2AP fluorescence is due to rapid charge transfer to neighboring bases (*2*−*5*), the rate of which should be highly dependent on the extent of π-orbital overlap. The dependence of the 2AP quenching rate on redox driving force in complexes of 2AP with native bases suggests that quenching occurs via hole transfer from 2AP to neighboring purines and by electron transfer to neighboring pyrimidines (*2*). This view is supported, in large measure, by recent TDDFT studies of the electronic structure of stacked DNA dimers and trimers containing a single 2AP (*3*, *4*). The theoretical studies, however, also indicate in the case of 2AP stacking with purines that extensive mixing of localized and charge transfer (CT) excitations occurs, such that the initially excited state already has some CT character.

Free 2AP in solution (pH 7) has a single isotropic fluorescence decay lifetime of 10.4 ns (*6*); incorporation of 2AP into an oligonucleotide or oligodeoxynucleotide duplex leads to heterogeneous fluorescence decays with time constants ranging from <50 ps to ∼10 ns (*6*−*10*). This heterogeneity is usually interpreted to report on a distribution of partially-stacked structures with the shortest component reflecting decay from the stacked conformations and the 8−10 ns components assigned to conformations where the 2AP is extrahelical (*6*, *7*). In a simple two-state, static conformational model, the fractional amplitude of the long component can be used to infer the relative populations of stacked and unstacked species.

In contexts where 2AP conformational fluctuations occur on time scales approaching the fluorescence time scale, a simple two-state model for relating decay amplitudes or fractional intensities to the extent of stacking is not valid. In these cases, the measured fluorescence decays will reflect a competition between the stacking−unstacking dynamics and the conformationally-dependent quenching rate. O'Neill and co-workers (*11*) have recently shown that 2AP motion in duplex DNA occurs over a range of time scales and that conformational fluctuations modulate ("gate") charge transfer between 2AP and neighboring bases. Here, we report steady-state and time-resolved fluorescence lifetime and anisotropy measurements of trinucleotides ($^{5'}$dXp2APpY$^{3'}$) in which a

† This work was supported by ACS-PRF AC6-36506 (J.M.J.).

* To whom correspondence should be addressed. Tel: (314) 362-4523. Fax: (314) 362-7813. E-mail: jjean@wanda.wustl.edu and hall@bionmr3.wustl.edu.

[1] Abbreviations: 2AP, 2-aminopurine; r2AP, 2-aminopurine riboside; CD, circular dichroism; fwhm, full width at half-maximum.

10.1021/bi049701p CCC: $27.50
Published on Web 07/16/2004

central 2AP is flanked by pyrimidines and/or purines. The central 2AP in these "sandwich" trimers should be considerably more "floppy" than in duplex DNA or in duplexes with mismatched base pairs or across from abasic sites. Thus these trimers provide prototypical systems for investigating the influence of large conformational fluctuations on the dynamics of charge transfer in single-stranded regions of nucleic acids. The temperature dependence and viscosity dependence of the fluorescence properties of these trimers provide clear evidence for "gated" charge transfer and provide new information on the time scale of stacking−unstacking dynamics in single-stranded regions of nucleic acids.

MATERIALS AND METHODS

The $^{5'}$dXp2APpY$^{3'}$ (X, Y = A, T, or G) trimers were synthesized using phosphoramidites from Glen Research and purified by HPLC. Samples were prepared at concentrations of 4−5 μM determined by absorbance measurements using 7200 M^{-1} cm^{-1} for the extinction coefficient of 2AP at 305 nm (*12*) in 10 mM sodium phosphate buffer (pH = 7) containing 100 mM NaCl. Absorption spectra were measured on a Shimadzu UV160U spectrophotometer, and circular dichroism spectra were measured on a Jasco (J-715) spectropolarimeter equipped with a thermoregulated quartz cell.

Steady-state fluorescence spectra were measured using a PTI fluorometer equipped with a temperature-regulated sample compartment (±0.1 °C). Fluorescence quantum yields of r2AP and the 2AP trimers were determined by referencing the integrated intensity at a given temperature to that of r2AP at T = 25 °C measured under identical solution conditions [ϕ_{r2AP} = 0.68 (1)].

Picosecond fluorescence decay measurements were carried out using the time-correlated single photon counting method. The laser system was a 76 MHz mode-locked Ti:S oscillator (Coherent Mira 900F) pumped by a diode-pumped, frequency-doubled Nd:YVO_4 laser (Coherent Verdi-V10). When warranted (i.e., for solution conditions leading to long decay components), we used a divide by 10 pulse-picked beam (NEOS) to ensure sufficient excited state relaxation between pulses. The excitation wavelength (300 nm, vertically polarized) was obtained by frequency tripling the Ti:S fundamental. The excitation power, typically ≤1 mW, was focused onto the sample using a 50 mm quartz lens. The emission was collected by a 60 mm lens, passed through a polarizer, and focused onto a photon-counting photomultiplier tube (Hamamatsu 5773P-03) with a 75 mm lens. The anode pulse of the PMT provided the start pulse for the TAC. The stop pulse was obtained by splitting off ~10% of the excitation beam and focusing it onto a UV-sensitive Si:C photodiode (JEC 0.1). A short-wave pass filter (Melles-Griot SWP-400) was used to reject stray light and/or buffer fluorescence at wavelengths >400 nm, and a GG385 (Schott) filter was used to filter out the excitation and water Raman lines. The sample concentrations were identical to those used in the steady-state experiments. The sample was contained in a 10 mm × 10 mm quartz cell in a thermoregulated chamber. The fwhm of the instrument response function, determined using the light scattered by a dilute suspension of nondairy coffee creamer in water, was found to be ~160 ps. For each sample, decay curves were collected using 2048 channels (6.1 ps/channel) and terminated when 65536 (2^{16}) counts were obtained in the peak channel. Lifetimes were obtained by orienting the polarizer at the magic angle (54.7°) relative to the excitation polarization, and anisotropy decays were acquired by making separate measurements with the emission polarizer set to the vertical and horizontal positions. Buffer fluorescence accounted for ~1% of the total fluorescence counts and <2% of the counts in the peak channel and was not subtracted from the sample decays prior to analysis. Lifetime decay curves were analyzed by a standard nonlinear least-squares, iterative reconvolution algorithm (Picoquant) assuming a sum of exponentials decay law:

$$I(t) = \sum_i \alpha_i e^{-t/\tau_i} \quad (1)$$

where τ_i and α_i are the time constants and corresponding amplitudes, respectively. Anisotropies were constructed from the parallel [$I_{||}(t)$] and perpendicular [$I_{\perp}(t)$] decays according to

$$r(t) = \frac{I_{||}(t) - GI_{\perp}(t)}{I_{||}(t) + 2GI_{\perp}(t)} \quad (2)$$

where the G-factor is a measure of the polarization bias of the detection system. The value of G was determined using tail matching of the parallel and perpendicular decay curves and was found to vary from 0.97 to 1.07. The time-dependent anisotropy was constructed from the parallel and perpendicular intensity components and fit directly using an iterative reconvolution procedure assuming a nonassociative model with biexponential decay:

$$r(t) = \beta_1 e^{-t/\theta_1} + \beta_2 e^{-t/\theta_2} \quad (3)$$

where β_i is the limiting anisotropy of component i and θ_i is the corresponding rotational correlation time. The sum of the β_i's gives the zero time anisotropy, $r(0)$.

RESULTS

Trimer Structure

Circular Dichroism Measurements. Though single strands of nucleic acids can exhibit a high degree of stacking, they also have a large degree of flexibility. CD spectra (*13*, *14*) indicate that the ribotrinucleotide ApApA, for example, is highly stacked at pH 7 and 25 °C. To examine the effects of temperature on the stacking of the 2AP-containing trimers, CD spectra were recorded at 10 and 50 °C under identical solution conditions as used in the fluorescence studies (Figure 1). All spectra show a minimum at 260 nm, which for most trimers loses intensity with higher temperature (dTp2APpG is the exception). This CD signal is usually interpreted as a reflection of helical stacking of the bases, and so using the amplitude of the signal in the 260 nm region as a reporter of changes in the relative population of stacked species, the results suggest that each of the trimers exhibits measurable stacking over the entire temperature range. Notably, none of the spectra exhibit the canonical A-form (a positive ellipticity maximum at ~270 nm) or B-form (a null near 260 nm, with a broad positive peak at 280 nm and a negative ellipticity maximum near 250 nm) characteristics, indicating that their solution structures cannot be assigned to these structures. It is interesting to note that Johnson et al. have

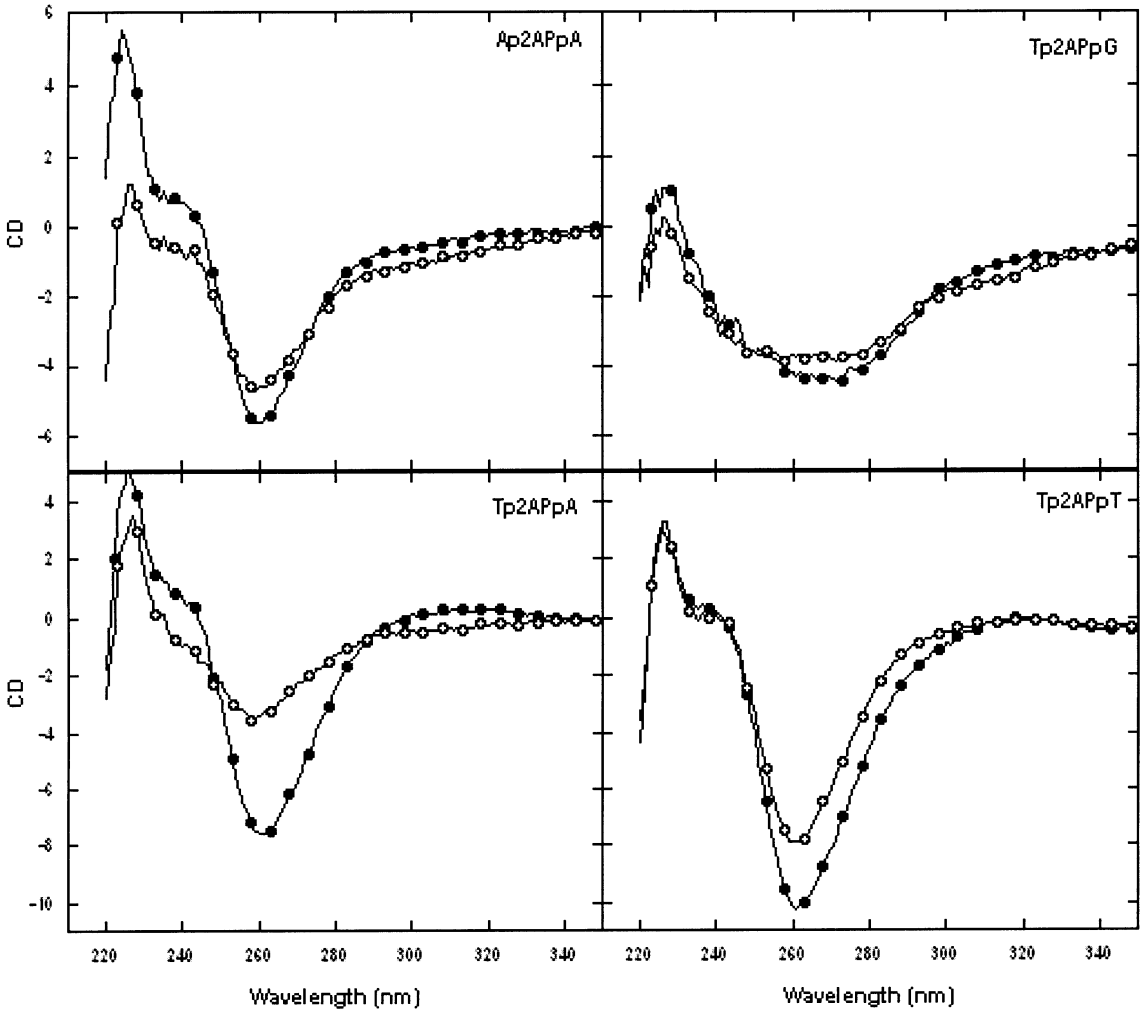

FIGURE 1: Circular dichroism spectra of 2AP sandwich compounds ($^{5'}$dXp2APpY$^{3'}$): $T = 10$ °C (solid circles); $T = 50$ °C (open circles). Sample concentrations were 10 μM (pH 7, 10 mM sodium phosphate, 100 mM NaCl).

recently used the CD signal from a 2AP dimer incorporated in a DNA duplex as a probe of the local conformation (*15*).

Steady-State Fluorescence Spectroscopy. The fluorescence absorption and fluorescence emission spectra of free r2AP, $^{5'}$dAp2APpA$^{3'}$, $^{5'}$dTp2APpA$^{3'}$, $^{5'}$dTp2APpG$^{3'}$, and $^{5'}$dTp2APpT$^{3'}$ at 25 °C are shown in Figure 2. The spectra have been scaled to the same absorbance at 305 nm and corrected for the wavelength dependence of the detector response. The incorporation of 2AP into a trimer leads to significant quenching of its fluorescence as is evident from Figure 2b. The fluorescence quantum yield as a function of temperature for r2AP and each trimer is shown in Figure 3. The yields of the trimer are similar to one another in magnitude but only ~3−9% of the yield of free r2AP at a given temperature. The purine-containing trimers show only weak temperature dependence of their fluorescence yields while the yield of dT2APT shows a 50% reduction over the range 10−70 °C. The decreasing yield of r2AP with increasing temperature reflects the increased rate of nonradiative decay of the $\pi-\pi^*$ state by internal conversion. The temperature dependence of the trimer yields, however, is context dependent.

In the special case of nucleic acids in which 2AP is flanked by an adenine, excitation into the adenine $\pi-\pi^*$ band results in energy transfer to 2AP. Nordlund and co-workers have shown that the observed ET efficiency serves as a sensitive measure of the extent of stacking and have used this observable to probe the dynamics of duplex melting (*16*) and conformations of single-stranded poly(dA) oligomers (*12*). Figure 4a shows the fluorescence excitation spectra for dAp2APpA at 10, 30, and 50 °C. Following Davis et al., the efficiency (E) of energy transfer is given by (*12*)

$$E = \frac{A_{2AP}(\lambda_{exc})}{A_A(\lambda_{exc})}\left[\frac{I_{trimer}(\lambda_{exc})}{I_{2AP}(\lambda_{exc})}\left(\frac{\phi_{2AP}}{\phi_{trimer}}\right) - 1\right] \qquad (4)$$

where A_{2AP} and A_A are the absorbances of the acceptor (2AP) and donor (A) in the trimer and I_{trimer} and I_{2AP} are the measured fluorescence intensities of the trimer and directly excited 2AP. ϕ_{2AP} and ϕ_{trimer} are the fluorescence quantum yields. The 2AP fluorescence intensity used in eq 4 is taken from measurements of the free r2AP; thus the ratio of fluorescence intensities appearing in the brackets is multiplied by the ratio of quantum yields to take into account the intrinsic difference in fluorescence yields between the trimer and the free nucleoside at a given temperature.

Figure 4b shows the calculated energy transfer efficiency as a function of temperature for dAp2APpA and dTp2APpA. As is apparent from comparing Figure 4b with the CD amplitudes at 260 nm (Figure 1), the ET efficiency has a steeper temperature dependence than does the CD signal, suggesting a higher sensitivity to changes in the distribution

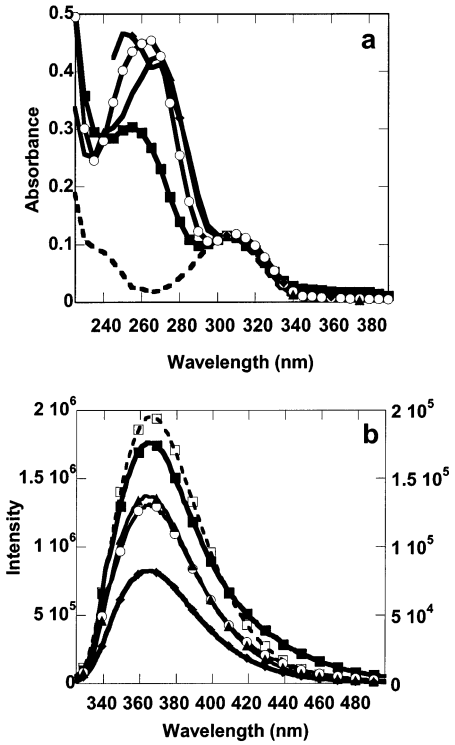

FIGURE 2: Absorption spectra (a) and emission spectra (b) of 2AP and 2AP sandwich compounds: $^{5'}$dAp2APpA$^{3'}$ (■), $^{5'}$dTp2APpA$^{3'}$ (○), $^{5'}$dTp2APpG$^{3'}$ (●), $^{5'}$dTp2APpT$^{3'}$ (▲), and r2AP (dashed line). For (b) the scale on the left-hand side corresponds to the r2AP spectrum. That on the right-hand side corresponds to the trimer spectra. Sample concentrations were ~4 μM (pH 7, 10 mM sodium phosphate, 100 mM NaCl).

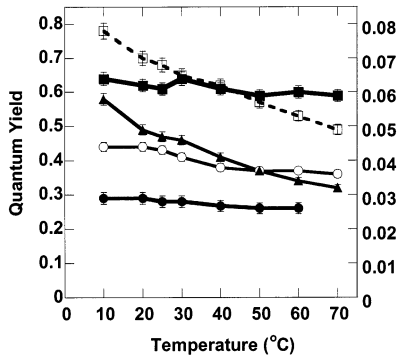

FIGURE 3: Fluorescence quantum yields as a function of temperature for r2AP (dashed line), $^{5'}$dAp2APpA$^{3'}$ (■), $^{5'}$dTp2APpA$^{3'}$ (○), $^{5'}$dTp2APpG$^{3'}$ (●), and $^{5'}$dTp2APpT$^{3'}$ (▲). The scale on the left-hand side corresponds to the r2AP data. That on the right-hand side corresponds to the trimer data. Error bars are estimated from five determinations of the quantum yield of r2AP.

of stacked conformations. Since the CD amplitude and ET efficiency arise from different electronic mechanisms with undoubtedly different sensitivities to the relative orientation of neighboring bases, this result is not surprising. Both sets of results clearly demonstrate that measurable stacking exists over the entire temperature range used in our fluorescence studies and that the distribution of stacked structures is temperature-dependent.

Trimer Dynamics

Fluorescence Decay Kinetics. The fluorescence quantum yield measurements, energy transfer efficiencies, and circular dichroism spectra report on an ensemble average over the

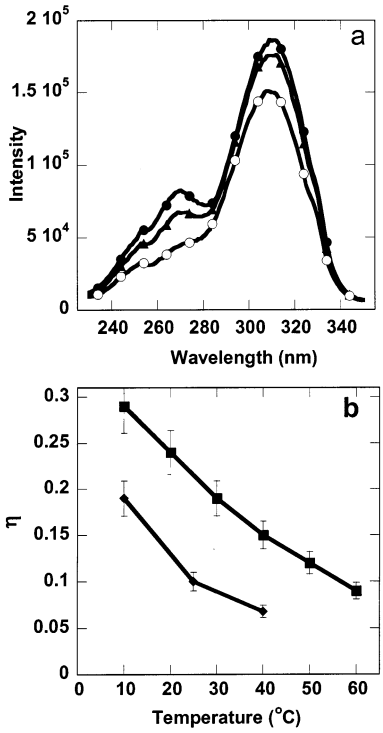

FIGURE 4: (a) Fluorescence excitation spectra of $^{5'}$dAp2APpA$^{3'}$ at T = 10 °C (●), 25 °C (▲), and 50 °C (○). (b) Energy transfer efficiency as a function of temperature for $^{5'}$dAp2APpA$^{3'}$ (■) and $^{5'}$dTp2APpA$^{3'}$ (●). Sample concentrations were ~4 μM (pH 7, 10 mM sodium phosphate, 100 mM NaCl).

distribution of stacked structures (the steady-state properties). They neither provide information on the extent of conformational heterogeneity nor indicate whether conformational exchange is static or dynamic on the fluorescence time scale. To address these issues, we have carried out time-resolved fluorescence lifetime studies as a function of temperature for each of the trimers. In all cases, the decays were adequately fit to three exponentials. In a few cases, the quality of the fit (as judged by the χ^2 value) was found to be marginally improved by addition of a fourth exponential. The value of the average lifetime, however, was not affected. The true nature of the ensemble is probably that of a (near) continuum of partially stacked structures. Attempts to model this continuum by fitting to a Gaussian distribution of decay rates did not give satisfactory results. The reported decay times from our discrete exponential fits thus serve only as an approximate gauge of the range of time scales of the dynamic processes contributing to the observed decay.

The decay parameters and intensity-weighted average lifetimes for all four trimers are shown in Table 1. Each trimer exhibits a wide range of decay times, ranging from <200 ps to ~3 ns, indicative of extensive conformational heterogeneity. The intensity-weighted lifetime provides a measure of the average time 2AP resides in the excited state. This average receives its dominant contribution from the longest component. The short components of the decay will be more heavily weighted in an amplitude-weighted average (not shown here), but our experimental apparatus is limited in its ability to resolve these components, given that its fwhm of the response function is ~160 ps. To test the ability of the decay model to accurately determine parameters on the order of the instrument response time, simulated decays composed of three exponentials with amplitudes and time

Table 1: Temperature Dependence of Fluorescence Decay Parameters[a]

trimer	T (°C)	α_1[b]	τ_1 (ns)[c]	α_2[b]	τ_2 (ns)[b]	α_3[b]	τ_3 (ns)[b]	$\langle\tau\rangle_{int}$[d]	χ_r^2
dAp2APpA	10	0.27	0.21	0.55	0.89	0.18	3.53	2.25	1.46
	20	0.33	0.17	0.52	0.79	0.15	3.23	1.97	1.48
	30	0.34	0.18	0.51	0.87	0.15	3.49	2.12	1.69
	40	0.35	0.14	0.49	0.81	0.16	2.94	1.74	1.64
	50	0.33	0.20	0.55	0.92	0.12	3.19	1.76	1.80
	60	0.33	0.17	0.57	0.91	0.10	3.03	1.58	1.83
dTp2APpA	10	0.36	0.15	0.46	0.69	0.18	3.99	2.85	1.42
	20	0.31	0.21	0.51	0.67	0.17	3.58	2.40	1.38
	30	0.32	0.12	0.50	0.59	0.18	2.96	2.03	1.45
	40	0.44	0.33	0.36	0.71	0.20	2.46	1.62	1.38
	50	0.54	0.34	0.31	0.84	0.16	2.13	1.29	1.49
	60	0.56	0.35	0.34	0.89	0.10	1.96	1.05	1.29
dTp2APpG	10	0.62	0.08	0.17	0.68	0.21	4.02	3.44	1.78
	20	0.54	0.09	0.23	0.67	0.23	3.41	2.81	1.70
	30	0.68	0.04	0.16	0.57	0.16	2.68	2.18	1.61
	40	0.65	0.05	0.19	0.52	0.16	2.05	1.61	1.44
	50	0.39	0.09	0.33	0.48	0.28	1.58	1.23	1.28
	60	0.32	0.09	0.35	0.41	0.33	1.17	0.92	1.48
dTp2APpT	10	0.70	0.05	0.13	0.73	0.17	3.52	2.98	1.87
	20	0.64	0.06	0.17	0.72	0.19	2.89	2.36	1.54
	30	0.68	<0.05	0.15	0.61	0.17	2.24	1.80	1.61
	40	0.67	<0.05	0.16	0.54	0.17	1.76	1.41	1.41
	50	0.80	<0.05	0.10	0.48	0.10	1.38	1.07	1.46
	60	0.86	<0.05	0.06	0.42	0.08	1.08	0.85	1.31

[a] Amplitudes are normalized such that $\sum\alpha_i = 1.0$. [b] Typical errors (obtained from support-plane analyses) are ±10% for amplitudes and ±15% for time constants. [c] Typical errors are +30%. [d] $\langle\tau\rangle_{int} = \sum_i\alpha_i\tau_i^2/\sum_i\alpha_i\tau_i$.

constants representative of those in Table 1 and containing Poisson random noise were generated and convoluted with the measured response function. Analysis of these simulated curves showed that components as short as 50 ps (with the amplitudes typically seen in our data) could be determined within 20−25% accuracy. It is probable that, in some cases, we are missing much shorter components. Larsen et al., using a streak camera with considerably better resolution than used here, found 2AP fluorescence components as short as 8−20 ps in their studies of a DNA hairpin when 2AP was flanked by a guanosine in either a stem or loop region (*10*).

The temperature dependence of the fluorescence decays is shown in Figure 5 for dAp2APpA and dTp2APpT. These two trimers display significant differences in their fluorescence quantum yields as a function of temperature and thus represent the complete range of photophysical behavior observed in our studies. The dAp2APpA fluorescence quantum yield is temperature-independent, whereas that of dTp2APpT drops by 50% over the 10−60 °C range. Both trimers show <200 ps decay components with substantial amplitudes that are nearly temperature-independent. The difference in the temperature dependence of the long time decay, however, is significant. The slow component of dAp2APpA varies from ~3.0 to 3.5 ns while that of dTp2APpT varies from ~1.2 to 3.5 ns over the same range.

In the case of dAp2APpA, increasing the viscosity of the environment has a pronounced effect on 2AP fluorescence time constants, as illustrated in Figure 6. These conditions span a nearly 10-fold range of viscosity over the temperatures of our experiments. In 60% glycerol at 10 °C, the shortest measured decay component is 0.46 ns compared to 0.20 ns in 0% glycerol, while the long component has increased from 3.5 ns (no glycerol) to 6.9 ns (60% glycerol). As a reference,

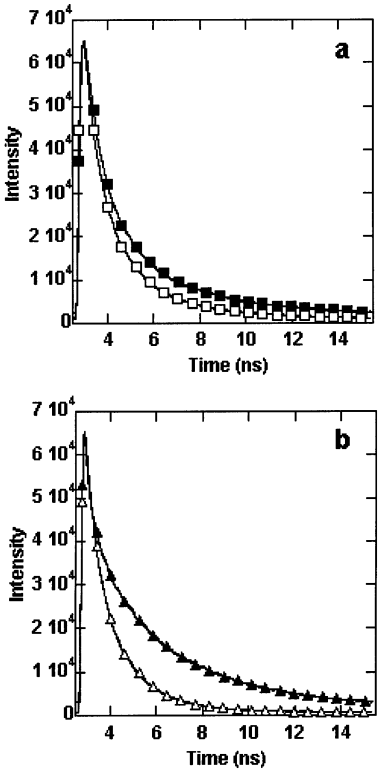

FIGURE 5: Fluorescence decays at $T = 10$ °C (solid symbols) and 50 °C (open symbols) for (a) $^{5'}$dAp2APpA$^{3'}$ and (b) $^{5'}$dTp2APpT$^{3'}$. Sample concentrations were ~4 μM (pH 7, 100 mM NaCl).

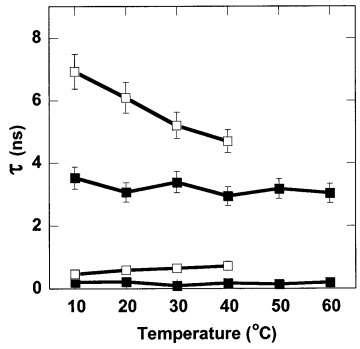

FIGURE 6: Temperature dependence of the shortest and longest time constants for the fluorescence decay of $^{5'}$dAp2APpA$^{3'}$ in 0% glycerol (■) and 60% (w/w) glycerol (□).

the lifetime of r2AP at 10 °C can be estimated from the quantum yield at the same temperature. Assuming only dynamic quenching is operable for the free r2AP, the ratio of the quantum yields at any two temperatures is equal to the ratio of the lifetimes. This is true, of course, only if the excited state decay is single exponential, which is the case for r2AP. Using the appropriate quantum yields and the reported lifetime at 25 °C (measured under identical solution conditions as here), the lifetime of r2AP at 10 °C is calculated to be ~12 ns. Thus, even at the highest viscosity examined, the value of the long decay component is still measurably less than that expected from an unstacked 2AP at the same temperature. The striking result is that the long decay component has developed a temperature dependence in the high viscosity solution.

Time-Resolved Anisotropies. Time-resolved anisotropy measurements provide a direct probe of the time scales of 2AP motion in the trimers (*8*, *17*). We have determined the

Table 2: Fluorescence Anisotropy Decay Parameters[a]

trimer	T (°C)	% glycerol[b]	β_1	θ_1 (ns)	β_2	θ_2 (ns)	$r(0)$	χ_r^2
dTp2APpG	10	0	0.13	0.11	0.16	0.49	0.29	1.10
	50	0	0.25	0.12	0.03	0.67	0.28	1.33
	10	60	0.07	1.2	0.24	4.6	0.31	1.30
dTp2APpA	10	0	0.10	<0.05	0.19	0.49	0.29	1.09
	50	0	0.21	<0.05	0.10	0.25	0.31	1.40

[a] Amplitudes are normalized such that $\sum\beta_i = r(0)$. [b] By weight.

anisotropy decays for dTp2APpA and dTp2APpG at 10 and 50 °C in 0% glycerol and for dTp2APpG at 10 °C in 60% glycerol. The decays were adequately fit with a two-component, nonassociated model, the parameters of which are shown in Table 2. The data indicate that, regardless of the experimental conditions, the fluorescence is virtually completely depolarized during the average fluorescence lifetime of the trimer. The initial value of the anisotropy ranges from 0.28 to 0.32; the theoretical maximum value is 0.40. Deviations from this [$r(0)$] value observed for the trimers are due to the presence of local 2AP motions too fast to be resolved in our experiment.

The anisotropy decays provide a direct measure of the rotational correlation times of 2AP in the trimer; however, they do not provide a direct measure of the time scale of changes in the relative orientation of 2AP and its stacking partners. If the stacking−unstacking motion were slow on the isotropic lifetime time scale, we would expect an anisotropy component that reflected the rigid tumbling of the trimer. Such motion would not couple to the quenching process since it does not alter the environment of the 2AP. We can estimate the rotational correlation time for a rigid trimer from the Debye−Stokes−Einstein equation ($\theta = \eta V/k_B T$, where η is the viscosity and V is the hydrodynamic volume). For a hydrated sphere with an anhydrous volume (815 Å^3) computed from a space-filling model for dTp2APpG and a typical hydration volume of 0.5 cm^3·g^{-1}, the rotational correlation time at 25 °C is ∼400 ps in 0% glycerol (∼1 cP) and 4 ns in 60% glycerol (∼10 cP). These values are comparable to those reported in Table 2. We note, however, that even at 10 °C there is considerable local motion of the 2AP relative to its neighbors as evidenced by the large amplitude of the ≤100 ps component.

The above analysis and interpretation should be viewed as only qualitative. The use of a nonassociated model for the anisotropy decay is probably not realistic since it assumes every isotropic component contributes to each anisotropy component. In addition, the inherent noise of anisotropy decay measurements and the rapid quenching place relatively large error bars on the measured amplitudes and decay times. Despite these caveats, the observation that even at low temperature the fluorescence from 2AP is largely depolarized on a time scale considerably shorter than that expected from a rigid, stacked structure indicates that substantial changes in the stacking of 2AP occurs on a time scale comparable to, or shorter than, that of the isotropic decay.

DISCUSSION

The fluorescence properties of 2AP in nucleic acids are commonly interpreted in terms of structural parameters. The observation of strong fluorescence quenching is a signature of extensive stacking of the 2AP. Time-resolved fluorescence

Scheme 1

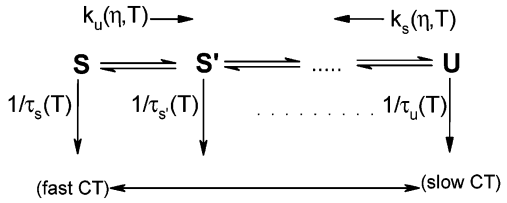

experiments of 2AP in duplexes show rapid decay components (10−500 ps) that are assigned to various stacked configurations. In contrast, time-resolved fluorescence studies of duplexes in which 2AP is paired with T or directly across from mismatched bases (8) or abasic sites (11) also exhibit a long lifetime component (5−20% amplitude) comparable to that of the free fluorophore. In environments where extensive conformational disorder of the 2AP base exists, such as loop regions of RNA (10) or DNA (8), free 2AP-like lifetime decay components are also present and account for a significant portion of the steady-state yield. The presence of these components indicates that 2AP spends a portion of its time extruded from the duplex structure, with no stacking on either neighboring base.

On the basis of previous observations, the extensive conformational disorder of a trimer should lead to long components in the decay and a relatively high quantum yield of dXp2APpY molecules. Instead, the absence of a free 2AP-like component in the time-resolved data suggests that significant fluctuations of the 2AP environment occur on the picosecond to nanosecond time scale in these systems. Rapid stacking−unstacking motions preclude the 2AP from surviving in an unstacked conformation long enough to exhibit its canonical lifetime of 10−12 ns. Thus, although at any given instant a substantial population of unstacked conformations may be present, rapid diffusion into a stacked structure followed by efficient charge transfer leads to a lower than anticipated fluorescence yield. The anisotropy data and effect of viscosity on the fluorescence decays also provide clear evidence that rapid conformational fluctuations of the 2AP occur and that these are strongly coupled to the quenching process. Thus the nonexponential fluorescence decay of the trimers reflects the dynamic competition between molecular motion and electronic decay. Given the lack of detailed information on the nature of the temperature-dependent stacking−unstacking free energy surface and the dependence of the quenching rate on the relative orientation of the bases, only a qualitative description of the dynamics can be gleaned from the data.

A Kinetic Model of Structure and Dynamics. The competition between conformational fluctuations [stacking (S)−unstacking (U) process] and the conformation-dependent quenching rate is easily seen from the simple multistate kinetic model shown in Scheme 1. The S, S′, etc. represent trimer conformations with distinct quenching (CT) rates. In this model we have assumed that only the nonradiative (CT) rate is conformationally dependent. The observed lifetime may also be influenced by stacking-induced changes in the radiative rate. Evidence for this comes from TDDFT studies that show, in the case of 2AP stacking with purines, the mixing of one or more CT transitions with the 2AP $\pi-\pi^*$ transition leads to a slight reduction in the radiative rate of the transition. On the basis of the wide range of time scales

observed for 2AP quenching in nucleic acids, we expect that the sensitivity of the overall decay rate results almost exclusively from stacking-induced changes in the CT rate.

Here k_s and k_u represent the overall stacking and unstacking rates, which depend on both temperature and viscosity, and $1/\tau_i$ denotes the conformation-dependent quenching rate. Under conditions where the overall stacking−unstacking rate is fast compared to the quenching rate of the optimally stacked state, the dynamic equilibrium of partially stacked structures in the kinetic scheme will be maintained during the decay of the 2AP excited state, and we would expect to see single-exponential decay with a rate that corresponds to the value of $1/\tau$ averaged over the equilibrium populations of the distinct conformations. In the opposite (static) limit, we would expect nonexponential decay with time constants that correspond to the individual intrinsic CT rates and amplitudes proportional to the equilibrium populations of these conformations. Experimentally, of course, the finite signal-to-noise ratio of the fluorescence signal yields a small number of discrete components that represent some "averaging" over the conformational continuum.

Our results suggest that these trimers are in an intermediate regime and that the time-resolved data reflect nonequilibrium ensemble dynamics. In such a case, the time scale of conformational exchange contributes to the measured decay. Following excitation, those structures that are substantially stacked result in a fast component in the decay, while the longer components correspond at least in part to the time scale of exchange between unstacked and stacked regions of the conformational free energy surface. That molecular dynamics contributes substantially to the decays is evident not only from the absence of a long component in the decay at any temperature but also in the viscosity dependence of the long component. Since the quenching rate from a given static conformation should be nearly independent of viscosity, the observation that increasing viscosity leads to substantial increase in the value of the time constant undoubtedly shows the influence of increased frictional effects on the stacking−unstacking transition.

Molecular motion near the lowest energy region of the free energy surface also contributes to fluorescence decay rates. Such conformational fluctuations account for the observation that the shortest measurable time scale in the decay of Ap2APpA *increases* with increasing viscosity at a given temperature. One plausible scenario is that the lowest energy conformation at a given temperature does not correspond to the fastest quenching rate. In this case, some molecular reorganization is needed to reach the optimally stacked configuration. Larsen et al. have posited a similar explanation for ~50−500 ps components observed in the loop regions of a 2AP-labeled DNA (*8*). A similar picture has been suggested by O'Neill and co-workers in their studies of 2AP-labeled DNA duplexes (*11*). These authors conclude that, even in the contexts where the conformational space of 2AP is restricted due to base-pairing and base-stacking interactions, ultrafast conformational fluctuations play a critical role in the transport of charge through DNA base stacks.

A computational study has also examined the structure and dynamics of the ApApA trimer (*18*). The stacking−unstacking free energy was determined via potential of mean force calculations at 25 °C along two reaction coordinates defined by the distances between the glycosidic nitrogens (N_9) of neighboring bases. The global minimum corresponds to a structure consistent with those seen in the experimental studies but also showed that a large number of conformational states, ranging from highly stacked to unstacked, were energetically accessible. The stacking−unstacking process in single-stranded oligomers is probably more complicated than suggested by the PMF calculations, since one can imagine relative motions of 2AP and one or both of its neighbors that substantially alter the π-overlap but do not lead to significant changes in the N_9-N_9 distance (e.g., rotations about the glycosidic bond). Inclusion of these types of motions in the definition of "unstacking" would seem to lead to a smaller effective barrier for unstacking. These in silico studies should be extended, using a metric for base stacking that includes a measure of the electronic structure of the dimer and trimer interactions.

CONCLUSIONS

A naive expectation of 2AP fluorescence in a simple trimer was that 2AP would exhibit the long time scale fluorescence decay and rapid anisotropy typical of the free nucleoside in solution, as a result of the flexibility of bases. What is observed, however, is that the dynamics of the structures lead to rapid fluorescence decay through transient stacking of the 2AP with its adjacent bases. We propose that charge transfer between 2AP and its stacking partners occurs rapidly and efficiently in one (or several) structure(s) in the trimer (a "sink" region), which is repeatedly accessed during rapid excursions of 2AP within its allowed conformational space. The results presented here provide strong evidence for the coupling of conformational fluctuations and charge transfer in the context of a highly dynamic local environment. On the basis of the observed fluorescence lifetimes on these molecules, a physical picture of the trimers involves motions of the bases on a picosecond to nanosecond time scale.

REFERENCES

1. Ward, D. C., Reich, E. S., and Stryer, L. (1969) Fluorescence studies of nucleotides and polynucleotides, *J. Biol. Chem. 244*, 1228−1237.
2. Wan, C., Fiebig, T., Schiemann, O., Barton, J. K., and Zewail, A. Z. (2000) Femtosecond direct observation of charge transfer between bases in DNA, *Proc. Natl. Acad. Sci. U.S.A. 97*, 14052−14055.
3. Jean, J. M., and Hall, K. B. (2001) 2-Aminopurine fluorescence quenching and lifetimes: Role of base stacking, *Proc. Natl. Acad. Sci. U.S.A. 98*, 37−41.
4. Jean, J. M., and Hall, K. B. (2002) 2-Aminopurine electronic structure and fluorescence properties in DNA, *Biochemistry 41*, 13152−13161.
5. O'Neill, M. A., Dohno, C., and Barton, J. K. (2004) Direct chemical evidence for charge transfer between photoexcited 2-aminopurine and guanine in duplex DNA, *J. Am. Chem. Soc.* (in press).
6. Guest, C. R., Hochstrasser, R. A., Sowers, L. C., and Millar, D. P. (1991) Dynamics of mismatched base pairs in DNA, *Biochemistry 30*, 3271−3279.
7. Nordlund, T. M., Andersson, L., Nilsson, L., Rigler, R., Gräslund, A., and McLaughlin, L. W. (1989) Structure and dynamics of a fluorescent DNA oligomer containing the *Eco*RI recognition sequence: Fluorescence, molecular dynamics, and NMR studies, *Biochemistry 28*, 9095−9103.
8. Larsen, O. F. A., van Stokkum, I. H. M., Gobets, B., van Grondelle, R., and van Amerongen, H. (2001) Probing the structure and dynamics of a DNA hairpin by ultrafast quenching and fluorescence depolarization, *Biophys. J. 81*, 1115−1126.
9. Rachofsky, E. L. Seibert, E., Stivers, J. T., Osman, R., and Ross, J. B. A. (2001) Conformation and dynamics of abasic sites in

DNA investigated by time-resolved fluorescence of 2-aminopurine, *Biochemistry 40*, 957−967.
10. Hall, K. B., and Williams, D. J. (2004) Dynamics of the IRE RNA hairpin loop probed by 2-aminopurine fluorescence and stochastic dynamics simulations, *RNA 10*, 34−47.
11. ONeill, M. A., Becker, H.-C., Wan, C., Barton, J. K., and Zewail, A. H. (2003) Ultrafast dynamics in DNA_mediated electron transfer: Base gating and the role of temperature, *Angew. Chem., Int. Ed. 42*, 5896−5900.
12. Davis, S. P., Matsumura, M., Williams, A., and Nordlund, T. M. (2003) Position dependence of 2-aminopurine spectra in penta-deoxynucleotides, *J. Fluoresc. 13*, 249−259.
13. Leng, M., and Felsenfeld, G. (1966) A study of polyadenylic acid at neutral pH, *J. Mol. Biol. 15*, 455−466.
14. Brahms, J., Micelson, A. M., and van Holde, K. E. (1966) Adenylate oligomers in single- and double-strand conformation, *J. Mol. Biol. 15*, 467−488.
15. Johnson, N. P., Baase, W. A., and von Hippel, P. H. (2004) Low-energy circular dichroism of 2-aminopurine dinucleotide as a probe of local conformation of DNA and RNA, *Proc. Natl. Acad. Sci U.S.A. 101*, 3426−3431.
16. Nordlund, T. M., Xu, D., and Evans, K. O. (1993) Excitation energy transfer in DNA: Duplex melting and transfer from normal bases to 2-aminopurine, *Biochemistry 32*, 12090−12095.
17. Rai, P., Cole, T. D., Thompson, E., Millar, D. P., and Linn, S. (2003) Steady-state and time time-resolved fluorescence studies indicate an unusual conformation of 2-aminopurine within ATAT and TATA duplex DNA sequences, *Nucleic Acids Res. 31*, 2323−2332.
18. Norberg, J., and Nilsson, L. (1996) Conformational free energy landscape pf ApApA from molecular dynamics simulations, *J. Phys. Chem. 100*, 2550−2554.

BI049701P